FLASH: new opportunities for (time-resolved) coherent imaging of nanostructures

2010 New J. Phys. 12 035015

(http://iopscience.iop.org/1367-2630/12/3/035015)

New Journal of Physics
The open-access journal for physics

FLASH: new opportunities for (time-resolved) coherent imaging of nanostructures

R Treusch[1] **and J Feldhaus**

Hamburger Synchrotronstrahlungslabor HASYLAB at Deutsches Elektronen-Synchrotron DESY, Notkestr. 85, D-22607 Hamburg, Germany
E-mail: rolf.treusch@desy.de

New Journal of Physics **12** (2010) 035015 (13pp)
Received 9 November 2009
Published 31 March 2010
Online at http://www.njp.org/
doi:10.1088/1367-2630/12/3/035015

Abstract. FLASH (free electron laser in Hamburg) is a unique, ultra-brilliant soft x-ray source providing highly coherent femtosecond pulses, currently in a wavelength range of 6.8–47 nm. Up to several 10^{12} coherent photons within a 10–70 fs pulse allow the study of dynamical changes in nanometer-sized structures. This is a big step towards the ultimate goal of observing femtosecond dynamics on the atomic length scale, for example 'watching bio-machines at work'. In this review, the properties of FLASH are summarized with a focus on coherence, and the potential of FLASH for structural investigations is illustrated with an overview of the recently performed coherent imaging experiments.

Contents

[1] Author to whom any correspondence should be addressed.

1. Introduction

Free electron lasers (FELs) are currently gearing up for becoming the brightest x-ray sources on earth. With their extremely brilliant femtosecond pulses and a wide wavelength range down to the ångström regime, vast areas of scientific terra incognita are now being entered. In the short-wavelength regime from the extreme ultraviolet (XUV) to the x-ray range, that is, from about 10 nm to 1 Å, FELs are on the verge of enabling 'movies' of chemical reactions, probing matter under extreme conditions, watching magnetic spins flip in real time, and unravelling the hitherto inaccessible structure of non-crystallizable biomolecules and following their functional dynamics. What was partially 'wild dreams' or almost science fiction just two decades ago now takes shape.

FLASH [1, 2] at DESY was the first FEL worldwide that opened the door to a bright future. Since 2005, when FLASH started user operation, we have seen many examples of scientific breakthroughs [3]. In the current wavelength range from 47 nm down to 6.8 nm,[2] FLASH possesses unprecedented properties, such as an extreme peak brilliance, femtosecond pulses and a high degree of coherence (cf sections 2 and 3). For the investigations of nanostructures and in particular their femtosecond dynamics, short-wavelength FELs in combination with the coherent diffractive imaging techniques described in this paper are superior to visible laser applications owing to the much higher spatial resolution achievable. Compared to short-pulse electron microscopy, one profits from a larger penetration depth and a better image contrast. In the XUV and soft x-ray range, FELs are complemented by 'table-top x-ray lasers' based on different technical approaches employing optical lasers [4]–[6]. Even though they are typically 2–4 orders of magnitude less intense than FELs, these table-top devices are suitable for various applications in the XUV (see for example [6]–[8]), being at the same time an affordable and compact laboratory solution. On the other hand, when it comes to ångström wavelengths and near-atomic resolution, the x-ray FELs are clearly unrivaled.

2. FELs from the coherence point of view

Besides short pulse lengths on the order of 10–100 fs and an unsurpassed peak brilliance of 10^{30}–10^{34} photons s^{-1} $mrad^{-2}$ mm^{-2} 0.1% bandwidth^{-1} (for soft x-rays to hard x-rays, respectively), FELs also possess a laser-like degree of coherence. FLASH, as well as all the x-ray FELs [9]–[11], is operated in the SASE (self-amplified spontaneous emission) [12] mode in which spontaneous undulator radiation is amplified to saturation in a single pass of an electron bunch through a long undulator. At the onset of saturation, the FEL pulses are characterized by one dominating transverse TEM_{00} mode and a few to several tens of longitudinal modes with longitudinal coherence lengths in the micrometer range [12]–[15]. In the future, full longitudinal coherence down to the x-ray range with coherence lengths up to a few hundred micrometers can be achieved via so-called self-seeding [16]. A corresponding technical realization is in progress at FLASH ([17] and references therein). Another approach yielding full longitudinal coherence is seeding via an external high-harmonic generation (HHG) laser. This concept will shortly be tested at FLASH via seeding at 35 and 13 nm wavelength. The required components are currently installed within the 'sFLASH' (see e.g. [18]) project. Compared to self-seeding, sFLASH also aims at Fourier-limited longitudinal coherence but

[2] This refers to the fundamental, which after a presently performed energy upgrade will reach down to below 5 nm.

potentially exhibits an order of magnitude shorter pulses (around 20 fs) at correspondingly wider spectral bandwidth ($\Delta\lambda_{ph}/\lambda_{ph} \leqslant 1\%$). In contrast to self-seeding, external seeding is currently limited to the XUV range since sufficiently intense (laser-based) seed sources are not available below 10 nm wavelength.

A figure of merit for the coherence of a radiation source is the so-called degeneracy parameter δ, which is the number of photons per mode. For an FEL it can be expressed as [14]

$$\delta = \dot{N}_{ph}\tau_c\zeta, \tag{1}$$

where $\dot{N}_{ph}$ is the photon flux, τ_c is the coherence time and ζ is the degree of transverse coherence.

The peak brilliance B_r of the radiation is defined as transversely coherent spectral flux:

$$B_r = \frac{\omega \mathrm{d}\dot{N}_{ph}}{\mathrm{d}\omega} \frac{\zeta}{(\lambda_{ph}/2)^2}, \tag{2}$$

where λ_{ph} is the photon wavelength and ω the corresponding frequency.

For a Gaussian spectral line, this yields

$$B_r = \frac{4\sqrt{2}c}{\lambda_{ph}^3}\delta \tag{3}$$

with the speed of light c, or put the other way round

$$\text{No. of photons per mode} = \text{Peak brilliance} \times \frac{\lambda_{ph}^3}{4\sqrt{2}\,c}. \tag{4}$$

Regarding the number of photons per mode, FELs are about 6–8 orders of magnitude superior to synchrotron radiation from undulators at storage rings where the coherent fraction of the beam has to be cut out via appropriate apertures or pinholes, respectively and spectral filtering. This is particularly visible in the hard x-ray regime where the number of photons per mode at a synchrotron radiation undulator drops below 1 since it scales with λ_{ph}^3 (equation (4)). For this reason, synchrotron radiation with its low number of coherent photons in a single pulse is not applicable for sub-100 ps time-resolved coherent imaging. On the other hand, the extremely brilliant FEL radiation allows us to obtain a high-resolution, low-noise diffraction image of a sample in a single, few-femtosecond shot before the sample—in most cases—disintegrates in a Coulomb explosion [19]. The coherent femtosecond pulses hold the promise that imaging of, for example, biological samples beyond conventional radiation damage resolution limits and in particular single-particle imaging at near-atomic resolution will be feasible once entering the x-ray wavelength range with FELs. The latter has been achieved at the Linac Coherent Light Source (LCLS) in Stanford recently [9] and we are looking forward to some more great scientific results here and at the European XFEL [10] as well as at the Japanese SCSS [11], both gearing up.

3. Properties of the FEL radiation pulses from FLASH

The properties of the XUV to soft x-ray FEL radiation produced by FLASH have been extensively characterized in the past, both with theoretical [20, 21] and experimental focus [1], [22]–[29]. The measured transverse coherence properties for some specific operation conditions are given in [25, 29]. In the aforementioned publications, longitudinal pulse properties such as coherence length and overall pulse length have been either inferred from

Table 1. Current operation parameters of FLASH and characteristic pulse properties (in or close to the saturation regime).

Property	Value	Comment
Wavelength (fundamental)	47–6.8 nm	The shortest λ_{ph} used in an experiment so far is 1.6 nm (the 5th harmonic of 8 nm)
Average pulse energy	10–100 μJ	Typically around 30–50 μJ
Bandwidth $\Delta\lambda_{ph}/\lambda_{ph}$ (FWHM)	0.7–1 %	
Pulse duration (FWHM) in general	70–10 fs	Derived from statistics/spectra; shorter for short wavelengths
Pulse duration (FWHM) measured	(29 ± 5) fs	At 23.9 nm [31]
	(35 ± 7) fs	At 13.5 nm [33]
Temporal coherence length (FWHM)	12 fs	At 23.9 nm [30]
	8.1 fs	At 33.2 nm [32]
Peak power	1 –5 GW	
Peak spectral brilliance	10^{29}–10^{30}	Photons s^{-1} $mrad^{-2}$ mm^{-2} 0.1% bandwidth^{-1}
Source size (FWHM)	100–200 μm	Depending on electron beam size
Source divergence (FWHM)	$\leqslant$100 μrad	Smaller for the short-wavelength end
Distance from source to sample	Around 70 m	

measurements of the pulse-to-pulse statistics together with the underlying FEL theory or estimated from the measured spectral width. Just recently, both the pulse length and the longitudinal coherence length have been measured as well. Different approaches have been used for that: two based on autocorrelation [30]–[32] and another one adopting cross-correlation concepts from attosecond metrology [33]. Table 1 summarizes the FLASH pulse properties. An overview of the FLASH user facility and its infrastructure for the broad spectrum of experiments [3] can be found in [2].

At FLASH, the number of coherent photons in a single mode ranges from a few times 10^{11} per pulse at the short wavelength end to a few times 10^{12} per pulse at longer wavelengths or, in other words, about 10 μJ per pulse independent of λ_{ph}. Since FLASH in the present, so-called 'femtosecond mode of operation' [21] typically exhibits only 1–2 transverse modes and 3–4 longitudinal modes, neither spatial nor spectral filtering is required to obtain good-quality pictures in the imaging experiments that will be described in the following.

4. Soft x-ray imaging experiments at FLASH

The science programme at FLASH covers a broad range of novel applications [3] including fundamental studies on atoms, ions, molecules and clusters, creation and characterization of warm dense matter, diffraction imaging of nanoparticles, spectroscopy of bulk solids and surfaces, investigation of surface reactions and spin dynamics, and the development of advanced photon diagnostics and experimental techniques. Among all those experiments, about a dozen imaging experiments have been performed at FLASH since 2005. They can be roughly grouped into five categories: coherent x-ray diffraction imaging (CXDI) [34]–[38],

in-line-holography (ILH) [38, 39], Fourier-transform-holography (FTH) [36, 38, 40], coherent x-ray resonant magnetic scattering (XRMS, partially time-resolved) [41]–[43] and time-resolved CXDI ('pump–probe') [44, 45] experiments.

4.1. Technical approaches

The main idea behind all the applied concepts for diffraction experiments at FLASH is to circumvent the problems of x-ray optics (such as short focal lengths—and consequently short working distances, absorption and optics damage) by working completely lensless. The spatial resolution of lensless imaging is, then, obviously not affected by limits of lenses either. Since the techniques are well established, they will be sketched only briefly here in order to work out the main differences between them. For a more detailed treatment, the reader is kindly referred to [46]–[48] and references therein. Schematic drawings comparing CXDI, ILH and FTH can be found in this focus issue [38].

CXDI is the basic approach where one illuminates a finite object with a coherent pulse yielding a diffraction pattern at a two-dimensional detector. For CXDI, the full, focused photon beam is impinging on the sample resulting in the highest possible scattering intensities even at high q-values, that is, at the outer edges of the detector. On the other hand, low-frequency information is often lost, since the high intensities need a considerably sized central beam stop to block the direct beam, which otherwise would saturate the detector. Furthermore, phase retrieval is somewhat more complicated than with the other methods described in the following. It needs more complex reconstruction algorithms, and assumptions about boundary conditions, for instance the shape of the frame supporting the sample, have to be made (see for example discussions in the Methods section of [34]). But solutions are at hand and then, after all, CXDI due to the absence of apertures bears the potential to produce high-quality, diffraction-limited images. Furthermore, with the high available flux at the sample it is the preferred tool for time-resolved single shot imaging. CXDI is also the method of choice for imaging injected particles 'on the fly', since the proper adjustment of the focal distance—for the specific particle that was hit—is handled computationally afterwards by the image reconstruction algorithms.

In the recent CXDI applications at FLASH, the beam size at the sample position—mostly in or close to the focus of the respective beamline—varied from a few microns to a few hundreds of microns. Beamstops for the direct, primary beam are put downstream of the sample in front of the detector/camera and are adapted to the specific beam size resulting from the experimental—in particular focusing—conditions. In the experiments by Chapman, Hajdu and others (see for example [34]–[36], [40, 45]) the 'beamstop' is often realized as a custom-made multilayer mirror that reflects the diffracted beam onto the CCD detector and lets the direct beam pass through a central hole (of around 1.2 mm diameter) in this mirror [49]. In another recent approach of that same collaboration, the camera detecting the diffracted beam is simply split into an upper and a lower half letting the direct beam pass through the gap in the middle. This allows adjusting the CCD halves to the minimum gap required to avoid saturation or damage of the detector by the direct beam while obtaining the maximum information at low q-values. In both the latter cases, the low-q limit typically corresponds to maximum probed length scales of one to a few microns, which is about the maximum sample size under study.

ILH uses a pinhole upstream of the sample as a spatial filter. This way, only a fraction of the coherent FEL beam is cut out in order to form a divergent wave front that illuminates the sample. Here the theoretical resolution limit is given by the effective numerical aperture coming

from the illumination of the detector by the central maximum of the Airy disc. In contrast to CXDI, low-frequency information about the scattering object is encoded in the hologram and is hence present in the reconstruction. ILH has a comparably large field of view and is hence best suited for imaging larger specimens of several 10 μm size.

Due to the gigawatt pulse power of FLASH, pinholes and/or filters required for ILH can obviously not be placed in a tightly focused and unattenuated beam. They are normally positioned out of focus and/or the beam is attenuated. The latter is done, for example, by using the spectrally resolved beam downstream of a monochromator or by applying thin (≈ 100 nm) absorber/filter foils or a gas attenuator [2] to absorb a substantial fraction of the XUV photons. Typical damage thresholds for the employed foil/pinhole materials are on the order of 100 mJ cm^{-2} [50, 51]. Thus, when the full beam is focused to a diameter below a few hundreds of microns, damage might occur already for a single FLASH pulse, whereas above 1 mm beam diameter, foils and pinholes typically even survive a multi-shot (long-term) exposure.

For the ILH experiments described in [38, 39] no beamstop was necessary since, due to the geometrical overillumination of the applied, about 1 μm diameter pinhole, the beam was attenuated by more than three orders of magnitude, reducing the flux at the sample to a few times 10^6 photons per pulse. That way, while avoiding saturation of the thinned, back-illuminated CCD detector behind the sample, the full low-frequency/low-q information could be preserved as well—but both at the expense of spatial resolution, since, due to the low intensities, averaging of images from many, fluctuating FEL pulses was required.

For **FTH**, the pinhole is not put in front of the sample but a pinhole or another reference object is present in the sample plane and imaged along with the sample. This very much facilitates phase retrieval since the obtained hologram is the convolution of the sample and the reference amplitudes. With the inherent reference, an inverse Fourier transform can be applied to the image, yielding a reconstruction of the (unknown) sample object in the best case down to a resolution of the finest resolvable structures of the reference scatterer. Note that also here, the low-frequency information is mostly absent due to the necessity of a central beam stop.

Coherent **XRMS** uses coherent illumination of a magnetic sample to record magnetic speckle images stemming from the magnetic domains. It resembles CDXI, apart from the fact that it is not the periodic arrangement of electrons, for example in a crystal lattice, that scatters, but the spatial magnetic correlations. Hence at FLASH wavelengths the diffraction image provides direct information on the magnetization density of the sample as well as on domain patterns.

Pump–Probe imaging: There is a large variety of setups for time-resolved experiments at FLASH, since different intense radiation sources, from FLASH itself across some dedicated optical lasers at the facility [52, 53] and user-owned lasers up to intense infrared and THz pulses [54], can be combined in single colour up to triple colour pump–probe configurations. For the coherent imaging experiments so far, the femtosecond magnetism dynamics were studied in an 'optical pump–XUV/soft x-ray (FLASH) probe' configuration [42, 43]. In the experiment by Gutt *et al* [42], single shot images of the magnetic sample have been recorded that allowed not only to track the time dependence of the magnetization density but also to follow the domain pattern of the magnetic multilayer on a picosecond timescale. A pump–probe imaging setup with slightly higher (mJ) pump-laser pulses was used for the explosions in the nanoworld by Chapman and co-workers [45]. Another experiment by Chapman *et al* [44] was inspired by Newton's 'dusty mirror' experiment [55] as it uses a (in this modern variant multilayer) mirror

behind the sample to back-reflect the same FLASH pulse again onto the sample. This makes up a soft x-ray *pump*–soft x-ray *probe* configuration where the initial diffraction from the sample (by the pump pulse) interferes with the diffraction produced by the same but delayed probe pulse to form a hologram of the explosion dynamics.

4.2. Studied samples

A large variety of samples have been studied in the intense FLASH pulses during the last years. Most groups started up with test patterns, often ion-beam etched in silicon nitride (Si_3N_4) membranes having a thickness of 100 nm or less. These were either non-periodic test patterns (for instance the famous 'two stick men below the sun' [34]) or periodic test patterns, so-called uniform redundant arrays (URAs)[3]. In a next step, a lot of particles of biological origin were imaged, such as large viruses, bacteria, picoplankton, etc, all typically in the size range from 100 nm to a few microns to adapt the objects under study to the available wavelengths and accordingly possible resolution at FLASH. Many of these biological samples instead of being fixed to the usual Si_3N_4 membrane were injected into the interaction zone (Chapman *et al*). In order to have frequent hits of particles in the beam by the coherent FLASH pulses, which could not really be synchronized with one another, the pulsed particle beam and the FLASH pulses were operated at high throughput and repetition rate, respectively. With improved injection schemes, the rate of imaging 'events' is now several Hz, at present being limited by the readout of the several megapixel 2D detectors [56]. The detector used by Chapman *et al* in this case was a recently developed, thinned, back-illuminated XUV-sensitive in-vacuum CCD camera, split into two halves as mentioned in section 4.1 [57]. The detector size is 16 megapixels, arranged as 4k × 4k pixels, often binned to 2k × 2k or smaller as a compromise between resolution and readout time. The large number of pixels results in readout times of fractions of a second—the state-of-the-art for the CCD technology, which is the usual approach for the XUV imaging experiments at FLASH. Within the framework of detector developments for the European XFEL, several projects, based on different technological approaches, are under way aiming for 2D megapixel detectors with parallel readout at MHz frame rates ([58] and references therein). This high readout rate, which is not achievable as yet, but probably within 5 years from now, is a requirement stemming from the non-equidistantly spaced ('burst-mode') pulse patterns of FELs based on superconducting linear accelerators.

For XRMS, magnetic samples were either periodic multilayers or crystals. Figure 1 gives an example of a single shot magnetic small angle scattering image [43].

Table 2 summarizes the results of all the coherent imaging experiments, regarding the applied imaging technique, samples, used wavelengths and achieved resolutions.

4.3. Technical developments

In order to illustrate the developments and achievements at FLASH along the way towards single molecule imaging at the upcoming x-ray FELs, the work of Chapman, Hajdu and coworkers during the last years may serve as an example (details can be found in the corresponding papers [34]–[36], [40, 44, 45] and in two summarizing publications [60, 61]).

The first studied samples were artificial structures (such as the 'stick men' [34]) that were milled into a 20 nm thin Si_3N_4 membrane with a focused ion beam (FIB). In parallel,

[3] URAs are also frequently used as 'reference beam generator' in the FTH setup sketched in section 4.1.

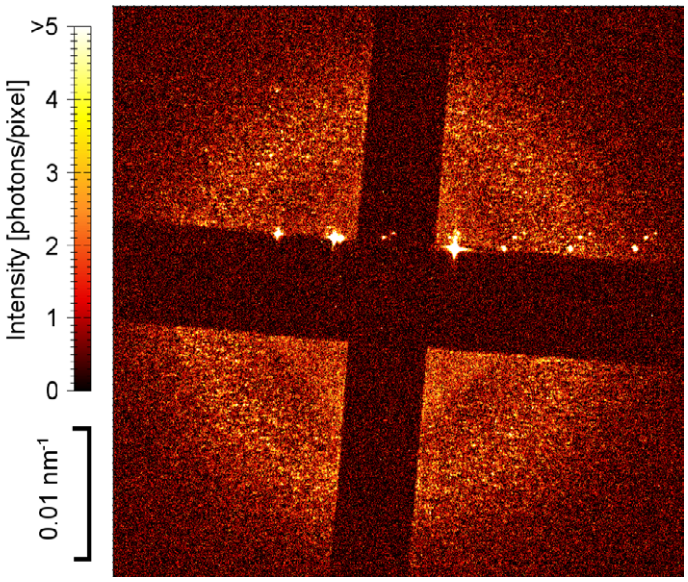

Figure 1. Resonant magnetic small-angle scattering (SAXS) pattern of labyrinth domains in a Co/Pd multilayer recorded with a single 20 fs FLASH pulse of 20 μJ energy. The photon energy was tuned to the Co M3-edge at 59.8 eV. After the pulse, the sample was destroyed. The maximum of the SAXS ring corresponds to a mean domain size of 230 nm. Due to the small sample aperture of 50 μm and the coherence of the FEL pulse, speckles appear in the scattering pattern. The intense directly transmitted beam and the scattering of the aperture edges was (mostly) blocked by two crossed 1 mm thick wires. The bright dots on top of the horizontal line of the shadow from this beamstop-cross are 'artefacts' that stem from scattered radiation going through some of the already exposed and hence destroyed membranes from other adjacent 'windows' of the array of samples on a wafer (Eisebitt *et al* [43]).

picoplankton and small bacteria on membranes were exposed to the FLASH pulses. Here, it was shown that placing a high-resolution reference pattern, for example an URA, side by side with the sample under study can significantly increase the resolution of the reconstructed sample image [36, 40]. Even if the sample itself only weakly scatters at higher q-values, the URA makes it an FTH setup and, in combination with iterative phase retrieval methods, the finally achieved resolution might even go beyond the resolution of the fabricated URAs (figure 2) [40].

Also around the same time, the first time-resolved experiments, both with a single colour XUV-pump/XUV-probe [44] as well as an optical laser-pump/XUV-probe [45], were performed and allowed to monitor explosions in the nanoworld.

As the next step, injected particles were investigated. Via an electrospray generator, an aerosol was produced, which was then expanded and guided through a differentially pumped aerodynamic lens into the vacuum system, yielding a beam of nanoparticles in a 'shotgun' mode [35, 60] (meaning particles flying at above 100 m s^{-1}, unsynchronized with the FLASH pulses). Just recently, another injection scheme with a micro-droplet source [62, 63] was employed. The latest significant breakthrough was single shot imaging of larger bacteria and viruses (200 nm to 2 μm size) on the fly [59].

Table 2. Summary of coherent imaging experiments at FLASH.

Method	Samples	Wavelength	Single or multi-pulse	Achieved resolution	Comment	Reference
CXDI	Test patterns in Si_3N_4 membrane (two stick men below sun)	32 nm	Single	62 nm	Diffraction limited	[34]
	DNA in sucrose balls (injected), average diameter 81 nm!	13.5 nm	Multi	$\leqslant$ 40 nm	Particles in free flight (first time); multi-pulse for 'hit-rate'	[35]
	2D periodic test pattern (2 μm and 495 nm periods in Si_3N_4 membrane)	8 nm	Multi (21 pulses)	$\leqslant$ 238 nm	Shows an alternative approach to single molecule imaging	[37]
	Latex spheres, Ag cubes, DNA nanocomplexes, picoplankton and lipid micelles (all injected)	13.5 nm	Multi	Not given	Multi-pulse to get high 'hit-rate'	[60]
	Mimiviruses, marine bacteriophages, bacterial cells, chromosomes, both injected and on Si_3N_4 membranes	7 nm	Multi and single	Under evaluation	Single pulse for fixed, multi-pulse for injected particles (hit rate)	[59]
CXDI + FTH	145 nm polystyrene spheres on Si_3N_4 membrane	32 nm	Single		Reference object substantially improves signal/background ratio	[36]
	+ reference object	13.5 nm	Single	40 nm		
Time-resolved CXDI	Latex balls on Si_3N_4 membrane	32.5 nm	Single (series)	62 nm	+holography	[44]
	Test patterns in Si_3N_4 membrane	13.5 nm	Single (series)	$\approx$50 nm	Time-resolution 10 ps	[45]
CXDI	Diatom cells (phytoplankton) on Si_3N_4 membrane	8 nm	Single	380 nm	CXDI resolution limited by detector size/geometry	[38]
+ ILH			Multi	$\approx$950 nm		
+ FTH			Multi	better than 450 nm		
ILH	SiO_2 particles and diatom cell on polymer window, rat embryonic fibroblast cells on Si_3N_4 membrane	8 nm	Multi (sum of 6300 p.)	620 nm		[39]
FTH	Bacterium + URA on/in Si_3N_4 membrane	13.5 nm	Single	150–75 nm	Image retrieved without input on reference object	[40]
Coherent XRMS	Co/Pd multilayer	1.59 nm	Multi (sum of 10^5 pulses)		5th harm. of 7.97 nm	[41]
	Co/Pt multilayer	20.8 nm	Single		Pump–probe	[42]
	Co/Pd multilayer	20.8 nm	Single + multi		Pump–probe	[43]

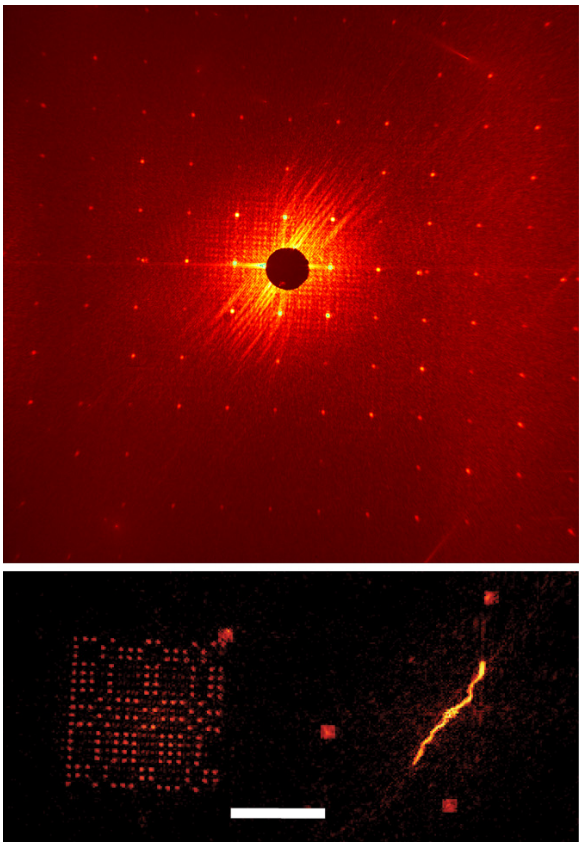

Figure 2. Ultrafast holographic imaging. Top: diffraction image from a bacterium (*Spiroplasma melliferum*) side by side with a URA. Bottom: reconstruction with iterative phase extension beyond the nanofabrication limit of the URA, which had 162 pinholes of 150 nm diameter each. The achieved resolution as deduced from the phase retrieval transfer function is around 75 nm (scale bar is 4 μm). Bottom left: URA; bottom right ('worm-like' bright structure): spiroplasma sample. The square bright spots originate from dust particles on the supporting Si_3N_4 membrane (see [40], in particular figure 3(a)).

Despite the great progress at FLASH as a source, all this would not have been possible without parallel development of a dedicated imaging and detection scheme [49], optimized injectors, such as the aerojet source [62], as well as next steps in the image reconstruction algorithms (see discussions in [36, 40]). Another key issue is to have reproducible objects at hand—which is easy, for instance, for the FIB-milled test patterns but needs more thought and work for 'real' samples such as picoplankton, bacteria and viruses. Having the samples, aligning them in order to allow summation of a series of images (as required, for example, in the case of weak scattering signals) is the next challenge. For simple molecules such as CO_2, laser alignment is already state of the art [64] and has recently been applied at FLASH as well [65]. More comments on this aspect of sample manipulation for the final goal of single biomolecule imaging can be found in [63]. There are clearly some more, in particular technical, challenges ahead of us.

5. Conclusions

We have seen significant advances in FEL technology over the last decade as well as continuous improvements on the experiment side concerning, in particular, sample preparation and manipulation, signal detection and data analysis, and last but not least, pump–probe techniques. All together, these are big steps forward on the road towards x-ray microscopy with femtosecond time resolution at interatomic length scales.

The recent results from FLASH demonstrate the steep learning curve on both the machine and the experiments side and give us great confidence that with the upcoming XFELs [9]–[11], it is only a matter of time to see, for instance, 'bio-machines at work'. Hence, with an even greater impact on a vast variety of scientific fields ranging from physics across materials science and chemistry to biology and medicine, a really bright future is yet to come [63].

Acknowledgments

Special thanks to the scientific and technical team at FLASH, in particular the machine operators and run coordinators, as they are the foundation for the successful operation of FLASH. We are indebted to Stefan Eisebitt and Henry Chapman for providing the figures of some recent results. RT has enjoyed participating in many of the research teams whose exciting scientific work is reviewed here.

References

[1] Ackermann W *et al* 2007 Operation of a free electron laser in the wavelength range from the extreme ultraviolet to the water window *Nat. Photonics* **1** 336–42

[2] Tiedtke K *et al* 2009 The soft x-ray free-electron laser FLASH at DESY: beamlines, diagnostics and end stations *New J. Phys.* **11** 023029

[3] http://hasylab.desy.de/facilities/flash/publications/selected_publications/
Bostedt C *et al* 2009 Experiments at FLASH *Nucl. Instrum. Methods* A **601** 108–22

[4] Suckewer S and Jaeglé P 2009 X-ray laser: past, present, and future *Laser Phys. Lett.* **6** 411–36

[5] Kato Y and Kawachi T 2009 Prospect of laser-driven x-ray lasers for extension to shorter wavelengths *Progress in Ultrafast Intense Laser Science IV (Springer Series in Chemical Physics* vol 91*)* ed K Yamanouchi, A Becker, R Li and S L Chin (Berlin: Springer) pp 215–32

[6] Ravasio A *et al* 2009 Single-shot diffractive imaging with a table-top femtosecond soft x-ray laser-harmonics source *Phys. Rev. Lett.* **103** 028104

[7] Sandberg R L *et al* 2008 High numerical aperture tabletop soft x-ray diffraction microscopy with 70-nm resolution *Proc. Natl Acad. Sci. USA* **105** 24–7

[8] Sandberg R L *et al* 2007 Lensless diffractive imaging using tabletop coherent high-harmonic soft-x-ray beams *Phys. Rev. Lett.* **99** 098103

[9] Emma P 2009 First lasing of the LCLS X-ray FEL at 1.5 Å Available at http://ssrl.slac.stanford.edu/lcls/commissioning/documents/th3pbi01.pdf; http://lcls.slac.stanford.edu/

[10] Altarelli M *et al* (ed) 2007 *The European X-Ray Free-Electron Laser: Technical Design Report* Report DESY 2006-097 (July 2007), available at http://www.xfel.eu/en/documents/; http://www.xfel.eu

[11] Shintake T *et al* 2008 A compact free-electron laser for generating coherent radiation in the extreme ultraviolet region *Nat. Photonics* **2** 555–9
http://www-xfel.spring8.or.jp/

[12] Saldin E L, Schneidmiller E A and Yurkov M V 1999 *The Physics of Free Electron Lasers* (Berlin: Springer)

[13] Saldin E L, Schneidmiller E A and Yurkov M V 2010 Statistical and coherence properties of radiation from x-ray free-electron lasers *New J. Phys.* **12** 035010

[14] Saldin E L, Schneidmiller E A and Yurkov M V 2008 Coherence properties of the radiation from X-ray free electron laser *Opt. Commun.* **281** 1179–88
[15] Saldin E L, Schneidmiller E A and Yurkov M V 2008 Output power and degree of transverse coherence of x-ray free electron lasers *Opt. Commun.* **281** 4727–34
[16] Feldhaus J, Saldin E L, Schneider J R, Schneidmiller E A and Yurkov M V 1997 Possible application of x-ray optical elements for reducing the spectral bandwidth of an x-ray SASE FEL *Opt. Commun.* **140** 341–52
[17] Treusch R *et al* 2007 Performance tests of the photon monochromator for self-seeding at FLASH *Proc. FEL2007 (Novosibirsk, Russia, August 2007)* pp 306–9, available at www.jacow.org/f07/PAPERS/WEBAU03.PDF
[18] Azima A *et al* 2008 sFLASH: an experiment for seeding VUV radiation at FLASH *Proc. FEL08 (Gyeongju, Korea, August 2008)* pp 405–8, available at http://accelconf.web.cern.ch/AccelConf/fel2008/papers/tupph072.pdf
[19] Neutze R, Wouts R, van der Spoel D, Weckert E and Hajdu J 2000 Potential for biomolecular imaging with femtosecond x-ray pulses *Nature* **406** 752–7
[20] The Test TESLA Facility FEL Team 2002 *SASE FEL at the Test TESLA Facility, Phase 2* Report DESY TESLA-FEL 2002-01 (June 2002), available at http://flash.desy.de/reports_publications/tesla_fel_reports/tesla_fel_2002/
[21] Saldin E L, Schneidmiller E A and Yurkov M V 2006 Statistical properties of the radiation from VUV FEL at DESY operating at 30 nm wavelength in the femtosecond regime *Nucl. Instrum. Methods* A **562** 472–86
[22] Andruszkow J *et al* 2000 First observation of self-amplified spontaneous emission in a free-electron laser at 109 nm wavelength *Phys. Rev. Lett.* **85** 3825–9
[23] Ayvazyan V *et al* 2002 Generation of GW radiation pulses from a VUV free-electron laser operating in the femtosecond regime *Phys. Rev. Lett.* **88** 104802
[24] Ayvazyan V *et al* 2002 New a powerful source for coherent VUV radiation: demonstration of exponential growth and saturation at the TTF free-electron laser *Eur. Phys. J.* D **20** 149–56
[25] Ischebeck R *et al* 2003 Study of the transverse coherence at the TTF free electron laser *Nucl. Instrum. Methods.* A **507** 175–80
[26] Ayvazyan V *et al* 2003 Study of the statistical properties of the radiation from a VUV SASE FEL operating in the femtosecond regime *Nucl. Instrum. Methods* A **507** 368–72
[27] Ayvazyan V *et al* 2006 First operation of a free-electron laser generating GW power radiation at 32 nm wavelength *Eur. Phys. J.* D **37** 297–303
[28] Düsterer S *et al* 2006 Spectroscopic characterization of vacuum ultraviolet free electron laser pulses *Opt. Lett.* **31** 1750–2
[29] Singer A, Vartaniants I A, Kuhlmann M, Duesterer S, Treusch R and Feldhaus J 2008 Transverse coherence properties of the free electron laser FLASH at DESY *Phys. Rev. Lett.* **101** 254801
[30] Mitzner R *et al* 2008 Spatio-temporal coherence of free electron laser pulses in the soft x-ray regime *Opt. Express* **16** 19909–19
[31] Mitzner R *et al* 2009 Direct autocorrelation of soft-x-ray free-electron-laser pulses by time-resolved two-photon double ionization of He *Phys. Rev.* A **80** 0235402
[32] Schlotter W F, Sorgenfrei F, Beeck T, Beye M, Gieschen S, Meyer H, Nagasono M, Föhlisch A and Wurth W 2010 Longitudinal coherence measurements of an extreme-ultraviolet free-electron laser *Opt. Lett.* **35** 372–4
[33] Frühling U *et al* 2009 Single-shot terahertz-field-driven x-ray streak camera *Nat. Photonics* **3** 523–8
[34] Chapman H *et al* 2006 Femtosecond diffractive imaging with a soft x-ray free-electron laser *Nat. Phys.* **2** 839–43
[35] Bogan M J *et al* 2008 Single particle x-ray diffractive imaging *Nano Lett.* **8** 310–6
[36] Boutet S, Bogan M J, Barty A, Frank M, Benner W H, Marchesini S, Seibert M M, Hajdu J and Chapman H 2008 Ultrafast soft x-ray scattering and reference-enhanced diffractive imaging of weakly-scattering nanoparticles *J. Electron Spectrosc. Relat. Phenom.* **166–167** 65–73

[37] Mancuso A P *et al* 2009 Coherent-pulse 2D crystallography using a free-electron laser x-ray source *Phys. Rev. Lett.* **102** 035502
[38] Mancuso A P *et al* 2010 Coherent imaging of biological samples with femtosecond pulses at the free-electron laser FLASH *New J. Phys.* **12** 035003
[39] Rosenhahn A *et al* 2009 Digital in-line holography with femtosecond VUV radiation provided by the free-electron laser FLASH *Opt. Express* **17** 8220–8
[40] Marchesini S *et al* 2008 Massively parallel X-ray holography *Nat. Photonics* **2** 560–3
[41] Gutt C *et al* 2009 Resonant magnetic scattering with femtosecond soft X-ray pulses from a free electron laser operating at 1.59 nm *Phys. Rev.* B **79** 212406
[42] Gutt C *et al* 2010 Single-pulse resonant magnetic scattering using a soft x-ray free-electron laser *Phys. Rev.* B **81** 100401
[43] Eisebitt S *et al* 2010 to be published
[44] Chapman H N *et al* 2007 Femtosecond time-delay X-ray holography *Nature* **448** 676–80
[45] Barty A *et al* 2008 Ultrafast single-shot diffraction imaging of nanoscale dynamics *Nat. Photonics* **2** 415–9
[46] Spence J C H 2007 Diffractive (lensless) imaging *Science of Microscopy* ed P W Hawkes and J C H Spence (New York: Springer)
[47] Eisebitt S 2008 X-ray holography: the hole story *Nat. Photonics* **2** 529–30
[48] Eisebitt S, Lüning J, Schlotter W F, Lörgen M, Hellwig O, Eberhardt W and Stöhr J 2004 Lensless imaging of magnetic nanostructures by X-ray spectro-holography *Nature* **432** 885–8
[49] Bajt S *et al* 2008 Camera for coherent diffractive imaging and holography with a soft-x-ray free-electron laser *Appl. Opt.* **47** 1673–83
[50] Hau-Riege S P *et al* 2007 Damage threshold of inorganic solids under free-electron-laser irradiation at 32.5 nm wavelength *Appl. Phys. Lett.* **90** 173128
[51] Hau-Riege S P *et al* 2009 Wavelength dependence of the damage threshold of inorganic materials under extreme-ultraviolet free-electron-laser irradiation *Appl. Phys. Lett.* **95** 111104
[52] Redlin H, Azima A, Stojanovic N, Tavella F, Düsterer S and Will I 2010 The FLASH pump–probe laser system in preparation
[53] Radcliffe P *et al* 2007 An experiment for two-color photoionization using high intensity extreme-UV free electron and near-IR laser pulses *Nucl. Instrum. Methods* A **583** 516–25
[54] Gensch M *et al* 2008 New infrared undulator beamline at FLASH *Infrared Phys. Technol.* **51** 423–5
[55] Newton I 1952 "*Opticks, or a Treatise of the Reflections, Refractions, Inflections & Colours of Light*", Book Two, Part IV (New York: Dover) (based on the 4th edition, first published by the Royal Society, London, 1730)
[56] Chapman H N and DePonte D P 2009 private communication
[57] *Custom-made CCD-camera from Xcam, UK* see http://www.xcam.co.uk/ and http://www.xcam.co.uk/documents/XCM_AP_237_1.pdf
[58] Graafsma H 2009 Requirements for and development of 2 dimensional x-ray detectors for the European X-ray Free Electron Laser in Hamburg *J. Instrum.* **4** 12011
[59] Chapman H N *et al* 2010 to be published
[60] Chapman H N *et al* 2009 Coherent imaging at FLASH *J. Phys.: Conf. Ser.* **186** 012051
[61] Chapman H N *et al* 2008 *Proc. 16th Conf. on Ultrafast Phenomena (UP 2008), Stresa (Italy)* (*Ultrafast Phenomena XVI* Springer Series in Chemical Physics vol 92) ed P Corkum, S De Silvestri, K A Nelson, E Riedle and R W Schoenlein (Berlin: Springer)
[62] DePonte D P, Weierstall U, Schmidt K, Warner J, Starodub D, Spence J C H and Doak R B 2008 Gas dynamic virtual nozzle for generation of microscopic droplet streams *J. Phys. D: Appl. Phys.* **41** 195505
[63] Chapman H N 2009 X-ray imaging beyond the limits *Nat. Mater.* **8** 299–301
[64] Stapelfeldt H and Seideman T 2003 Colloquium: aligning molecules with strong laser pulses *Rev. Mod. Phys.* **75** 543–57
[65] Johnsson P *et al* 2009 Field-free molecular alignment probed by the free electron laser in Hamburg (FLASH) *J. Phys. B: At. Mol. Opt. Phys.* **42** 134017